

## Surface Properties of LaCrO<sub>3</sub>

### Equilibrium and Kinetics of O<sub>2</sub> Adsorption

J. L. G. FIERRO AND L. GONZÁLEZ TEJUCA<sup>1</sup>

*Instituto de Catálisis y Petroleoquímica, C.S.I.C., Serrano 119, Madrid 6, Spain*

Received August 2, 1983; revised December 8, 1983

The equilibrium and kinetics of adsorption of oxygen on LaCrO<sub>3</sub> have been studied in a wide range of temperatures (77 to 777 K). Above 350 K activated adsorption occurs; in this region, rather low coverages of oxygen (below 0.20) were recorded. The exponential decrease of the isosteric heat of adsorption with coverage suggests that the surface of LaCrO<sub>3</sub> is heterogeneous. After heating at 1270 K in H<sub>2</sub> only a reduction of  $1.30 \times 10^{-2} e^-$  per molecule of LaCrO<sub>3</sub> was attained; this shows a high stability of the Cr<sup>3+</sup> ion in the perovskite structure. Concentration of hydroxyl groups after adsorption of H<sub>2</sub>O on the reduced sample was found to be higher than that on the oxidized one. The kinetic data (at pressure or temperature constant) were analyzed according to Elovich's equation. From semilogarithmic plots of the initial adsorption rate versus  $1/T$  an activation energy of adsorption of 16.4 kJ mol<sup>-1</sup> was calculated. LaCrO<sub>3</sub> was found to adsorb less oxygen and to be more difficult to reduce with H<sub>2</sub> than LaCoO<sub>3</sub>. This could account for the better catalytic properties of the latter for CO oxidation.

#### INTRODUCTION

Perovskite-type oxides are known to be catalysts for a number of reactions such as total and partial oxidation, hydrocracking, hydrogenation, hydrogenolysis, NO reduction, etc. Recent work carried out in this laboratory focused on the study of O<sub>2</sub>, CO, and CO<sub>2</sub> adsorption on LaMeO<sub>3</sub> oxides (1) and the catalytic activity of these compounds for CO oxidation (2).

Simple oxides which catalyze partial oxidation reactions do not adsorb significant amounts of oxygen while those which are catalysts for total oxidation are good adsorbents (3). Also, the profile for oxygen adsorption found by Iwamoto *et al.* (3) for first-row transition metal oxides (with two maxima for MnO<sub>2</sub> and CoO) is similar to the profile of catalytic activity for CO oxidation found in this laboratory (2) for LaMeO<sub>3</sub> oxides (Me = V, Cr, Mn, Fe, Co, and Ni). This seems to support the idea that catalytic activity for total oxidation processes

should be directly related to the amount of adsorbed oxygen.

In this work, equilibrium and kinetics of adsorption of O<sub>2</sub> on LaCrO<sub>3</sub> (with a low activity for CO oxidation) and the reducibility with H<sub>2</sub> of this oxide are studied. Kinetic data were analyzed according to the Elovich's equation. The equilibrium data are compared with those obtained for the system O<sub>2</sub>/LaCoO<sub>3</sub> (1). The large difference in catalytic activity for CO oxidation between LaCrO<sub>3</sub> and LaCoO<sub>3</sub> is discussed.

#### EXPERIMENTAL

**Materials.** As starting materials the compounds and gases used were La(NO<sub>3</sub>)<sub>3</sub> · 6H<sub>2</sub>O, Cr(NO<sub>3</sub>)<sub>3</sub> · 9H<sub>2</sub>O, and citric acid monohydrate, reagent grade from Merck. O<sub>2</sub> 99.98% pure and H<sub>2</sub> 99.995% pure both from Sociedad Española del Oxígeno; they were purified by standard methods.

**Sample preparation.** Following a method similar to that used by Johnson *et al.* (4), a sample of LaCrO<sub>3</sub> was prepared by freeze-drying (at 218 K) of an equimolecular solution of metal nitrates and evaporation in

<sup>1</sup> To whom all correspondence should be addressed.

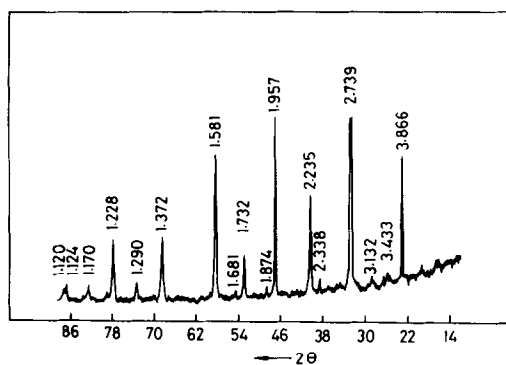


FIG. 1. X-Ray diffraction pattern (CuK $\alpha$  radiation) of a LaCrO<sub>3</sub> sample obtained from a freeze-dried precursor;  $d$  in Å (1 Å = 0.1 nm).

vacuum; the mixture of nitrates so obtained was then heated gradually in air up to 923 K, the product being kept for 80 h at this temperature. A second sample of lanthanum chromite was prepared by amorphous precursors decomposition as described by Courty *et al.* (5). Briefly, to an equimolecular solution of metal nitrates a solution of citric acid was added so that the ratio of gram · equivalents of citric acid to total gram · equivalents of metals was equal to 1. The water was evaporated in a rotary evaporator at 343 K and 10 mm Hg (1 mm Hg = 133.3 Nm<sup>-2</sup>) until the precipitate acquired the consistency of a viscous syrup. The precursor so obtained was kept in a vacuum stove at 373 K for 5 h and then heated gradually up to 1023 K (in air) this temperature being kept for 4 h. By means of thermal gravimetric and derivative thermal gravimetric analyses (heating rate, 5 K min<sup>-1</sup>) neither weight loss nor the appearance of new compounds were detected after further heating up to 1273 K (2). Both preparations gave similar X-ray diffraction patterns. In neither case peaks of simple oxides of lanthanum and chromium were observed. The lower temperature for formation of a single perovskite phase required by the freeze-dried precursor should be due to the highly homogeneous mixture of nitrates obtained by this method. As an example, in Fig. 1 a typical X-ray pattern of

one of the samples (freeze-drying) is shown. According to Tofield and Scott (6) the green-color LaCrO<sub>3</sub> so obtained should not exhibit oxidative nonstoichiometry although Voorhoeve *et al.* (7) indicate that a lanthanum chromite with excess of oxygen might be formed in the experimental conditions used in this work. In Table 1 some characteristics of these samples are given.

**Equipment and methods.** The experiments of adsorption of H<sub>2</sub>O, reducibility and kinetics of O<sub>2</sub> adsorption were carried out in a gravimetric system with a Cahn 2100 RG electrobalance (sensitivity 1  $\mu$ g). For sample reduction a Stanton Redcroft LVP/CA4/R temperature programmer was used. The experiments of equilibrium of adsorption of O<sub>2</sub> were carried out in a volumetric system with an MKS capacitance manometer for pressure measurements. The apparatus has a measuring range of 10<sup>-2</sup> to 10<sup>3</sup> mm Hg and a sensitivity of 10<sup>-2</sup> mm Hg (0.2  $\mu$ g O<sub>2</sub> or 3  $\times$  10<sup>15</sup> molecules). Both volumetric and gravimetric systems attained a dynamic vacuum of 10<sup>-6</sup> mm Hg. Infrared spectra were obtained with a Perkin-Elmer 682 spectrophotometer using a wedge attenuator in the reference beam and a cell with NaCl windows. X-Ray diffraction patterns were obtained with a Philips 1010 diffractometer using CuK $\alpha$  radiation.

Infrared spectra were obtained with oxidized (as prepared) and reduced (outgassing at 773 K for 4 h and then 300 mm Hg H<sub>2</sub>

TABLE 1

LaCrO<sub>3</sub> Samples

Experiment	Preparation method and final heating temperature (K)	Weight (g)	S <sub>BET</sub> (m <sup>2</sup> g <sup>-1</sup> )
ir spectra/H <sub>2</sub> O adsorption	Freeze-drying (923)	0.015/0.500	3.66
Equilibrium of O <sub>2</sub> adsorption	Freeze-drying (923)	1.917	3.66
Reducibility	Freeze-drying (923)	0.420	3.66
Kinetics of O <sub>2</sub> adsorption	Citrates decomposition (1023)	0.569	5.70

at 773 K for 1 h in a static system) samples. Self-supporting disks of 1-cm diameter made by pressing 15 mg of dry powder at  $2.7 \times 10^7 \text{ N m}^{-2}$  were used. After outgassing at 773 K for 4 h the temperature was lowered to 523 K and then the sample was contacted with 6 mm Hg of distilled  $\text{H}_2\text{O}$  for 1 h. Spectra were recorded after pumping at 393, 473, 573, 673, and 773 K for 2 h at each temperature. For the quantitative determination of OH groups the same kind of samples (oxidized or reduced powder) and the same procedure (adsorption of  $\text{H}_2\text{O}$  at 523 K and pumping at increasing temperatures) indicated for ir experiments were used. A reading in the electrobalance was made after constant weight was observed (usually after pumping for 10 min at each temperature).

Prior to an experiment of equilibrium of  $\text{O}_2$  adsorption the sample was outgassed in high vacuum at 773 K for 15 h; the temperature was then lowered to that of the experiment and the isotherm for total adsorption recorded; after pumping in high vacuum at the experiment temperature for 15 h, a second isotherm (reversible adsorption) was run. The system adsorbent-adsorbate was considered to be in equilibrium when the adsorption in 1 h was less than  $2 \times 10^{16}$   $\text{O}_2$  molecules per g of adsorbent.

In reduction experiments (static conditions, Table 3), the sample was heated in high vacuum at 4 K/min. After allowing 1 h at the reduction temperature,  $\text{H}_2$  (300 mm Hg) was let into the electrobalance enclosure and the weight change as a function of time recorded. In all cases, constant weight was reached in less than 1 h. Before starting the following experiment, the sample was reoxidized at 773 K for 1 h in air. For kinetic experiments the sample underwent the same initial outgassing (773 K, 15 h) above described; usually kinetic runs were recorded for 200 min. To avoid weight changes caused by thermomolecular effects, an initial zero reading in the electrobalance was determined by extrapolation of the initial part of the curve  $C_A$  (adsorbed

amount) vs  $t$  (time) at  $t = 0$ . Calculations of initial rates of adsorption (at constant temperature or pressure) were made by fitting the integral data to a polynomic function and analytic differentiation to  $t = 0$ . It was assumed that the gravimetric experiments occurred at constant pressure as the electrobalance volume ( $4 \text{ dm}^3$ ) is much larger than the volume of adsorbed gas.

## RESULTS AND DISCUSSION

### Surface Hydroxyl Groups

Infrared spectra in the OH stretching zone, obtained after  $\text{H}_2\text{O}$  adsorption at 423 K on the oxidized and on the reduced samples and pumping at increasing temperatures are given in Fig. 2. In both cases two bands at  $3680 \text{ cm}^{-1}$  of isolated OH groups (centers b) and at  $3550 \text{ cm}^{-1}$  (wide) of hydrogen-bonded OH (centers a) were observed. The O-H bond in this last case should be weaker and therefore these hydroxyls should be more acidic. Note that band intensities are stronger on the reduced sample.

In previous experiments of  $\text{H}_2\text{O}$ -pyridine adsorption on  $\text{LaCrO}_3$  (8) bands of Brønsted centers were observed only on the reduced sample (not on the oxidized

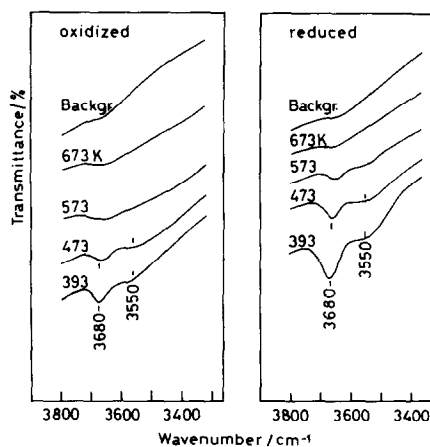
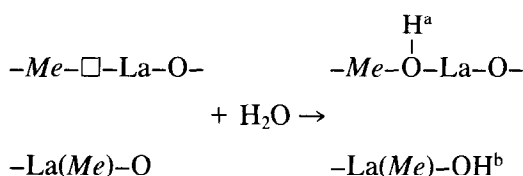


FIG. 2. Infrared spectra after  $\text{H}_2\text{O}$  adsorption at 423 K on oxidized and reduced  $\text{LaCrO}_3$  and pumping at increasing temperatures.

one). Pyridine probably does not react with centers b (basic) which are on the surface in higher concentration than centers a (acidic) as indicated by the stronger intensity of the 3680 cm<sup>-1</sup> band (Fig. 2). On the other hand, the pyridine molecule, because of its large size, may have not access to all acidic OH groups. This could explain the undetectability of ionizable hydroxyls by means of adsorption of this molecule.

In Fig. 3, gravimetric data obtained after H<sub>2</sub>O adsorption at 423 K on both oxidized and reduced samples and pumping between 400 and 800 K are given. The concentration of OH groups (considering that two OH are formed by one adsorbed H<sub>2</sub>O molecule) ranges between 6 and 0 OH nm<sup>-2</sup> being on the reduced sample larger, by about 1 OH nm<sup>-2</sup>, than that on the oxidized one. These concentrations are similar to these found by Crespin and Hall (9) after H<sub>2</sub>O adsorption at room temperature (r.t.) on BaTiO<sub>3</sub> and SrTiO<sub>3</sub> and heating in circulating He (with a liquid N<sub>2</sub> trap) between r.t. and 873 K.

These results can be accounted for assuming that the adsorption and dissociation of H<sub>2</sub>O takes place on pairs of surface acid-base centers, anion vacancy -O<sup>2-</sup>, according to the scheme:



yielding an acidic OH on an anion vacancy placed between coordinatively unsaturated La<sup>3+</sup> and reduced transition metal ions (Me<sup>2+</sup>, Me<sup>+</sup>) (center a) and a basic OH on a coordinatively unsaturated oxygen ion bonded to a La or Me ion (center b). Centers a and b should correspond to OH groups yielding bands at 3550 and 3680 cm<sup>-1</sup>, respectively. The fact that dissociation of H<sub>2</sub>O takes place on the oxidized sample suggests that pumping at 773 K generates anion vacancies on the surface although in low concentrations. The reduc-

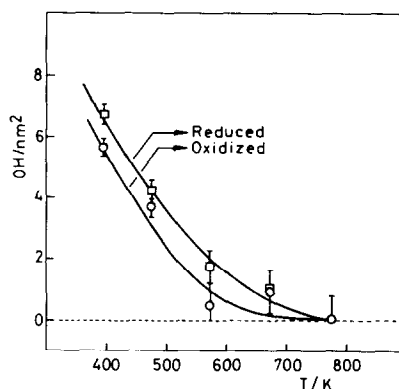


FIG. 3. OH concentration after H<sub>2</sub>O adsorption on oxidized and reduced LaCrO<sub>3</sub> as a function of the outgassing temperature.

tion steps greatly favors the formation of these vacancies.

No noticeable differences were observed by infrared spectroscopy (after H<sub>2</sub>O-pyridine adsorption) on reduced LaCrO<sub>3</sub> and reduced LaCoO<sub>3</sub> (oxidized LaCoO<sub>3</sub> presents too low transmission to ir radiation). However, OH concentration after H<sub>2</sub>O adsorption on LaCoO<sub>3</sub> and pumping above r.t. (9) are higher than these found for LaCrO<sub>3</sub> (Fig. 2).

### Equilibrium of Adsorption

Isotherms for total and reversible adsorption are given in Fig. 4. Below 273 K they are of type II while those above that temperature are of type I. The coverage for total adsorption ( $\theta_{\text{total}}$ , Table 2, taking as

TABLE 2  
Reversible ( $C_{A \text{ rev}}$ ) and Total ( $C_{A \text{ total}}$ ) Adsorption of O<sub>2</sub> at  $6.7 \times 10^3 \text{ N m}^{-2}$

	T (K)						
	77	195	273	381	474	570	677
$C_{A \text{ rev}}$ ( $10^{17} \text{ molec} \cdot \text{m}^{-2}$ )	59.9	1.68	0.28	0.59	0.65	1.57	8.14
$C_{A \text{ rev}}/C_{A \text{ total}}$	0.66	0.26	0.13	0.26	0.10	0.12	0.67
$\theta_{\text{total}}$	1.27	0.09	0.03	0.03	0.10	0.18	0.17

Note. For  $\theta_{\text{total}}$  (coverage for total adsorption) a cross-sectional area of O<sub>2</sub> molecule of 0.141 nm<sup>2</sup> was taken.

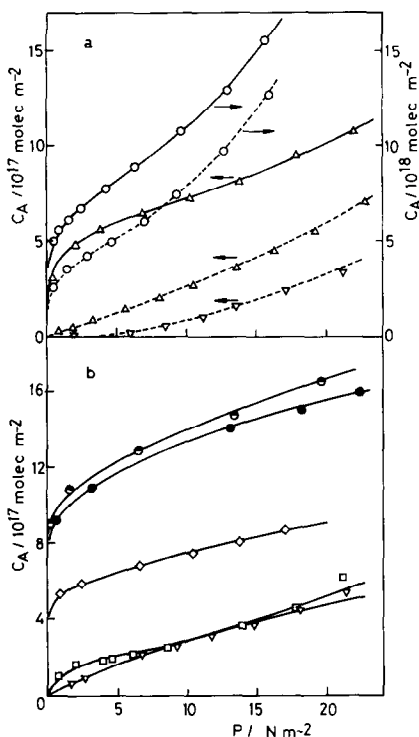


FIG. 4. Isotherms for total (—) and reversible (---) adsorption. (a)  $\circ$ , 77;  $\triangle$ , 195;  $\nabla$ , 273 K. (b)  $\nabla$ , 273;  $\square$ , 381;  $\diamond$ , 474;  $\bullet$ , 570;  $\bullet$ , 677 K.

cross-sectional area of  $O_2$  molecule  $0.141 \text{ nm}^2$  (10) recorded at 77 K indicates multilayer adsorption. Above 273 K, the low coverages and the small ratios  $C_{A \text{ rev}}/C_{A \text{ total}}$  observed (except that at 677 K), suggest that chemisorption is predominant.

In Fig. 5, the adsorption isobar at  $6.7 \times 10^3 \text{ Nm}^{-2}$  is plotted (for comparison the isobar for the system  $O_2/\text{LaCoO}_3$  given in a previous work (1) was also included). The above results suggest that the first descending branch should be associated mainly to physical adsorption while above 350 K activated adsorption occurs. The largely different times needed for completion of one isotherm (36 h at 273 K and 48–168 h for isotherms at 381–570 K) point also to the presence of an activation energy in this last temperature interval. The minimum temperature for overcoming the potential barrier should be situated around 600 K and this could account for the remarkably dif-

ferent amounts of reversible adsorption observed at 570 and 677 K (Table 2).

The isotherm of total adsorption at 77 K fitted satisfactorily the BET equation; from the adsorption at monolayer coverage a value of  $0.166 \text{ nm}^2$  for the cross-sectional area of  $O_2$  molecule was calculated. This is in reasonable agreement with that given by Emmett ( $0.141 \text{ nm}^2$ ) (10). The heat of adsorption in the first layer (calculated from the constant  $c$ ) was  $2.9 \text{ kJ mol}^{-1}$ .

The adsorption heats calculated by application of Clausius–Clapeyron equation to the reversible isotherms in the first descending branch of the isobar (195 to 273 K), of  $20 \text{ kJ mol}^{-1}$  and below (Fig. 6) are indicative of physical adsorption. Their exponential decrease with coverage (which suggests that the adsorbent surface is heterogeneous) corresponds to an adsorption process according to the Freundlich's model. However, as coverages for reversible adsorption observed at 195 K and above lie below 0.10, any extrapolation to

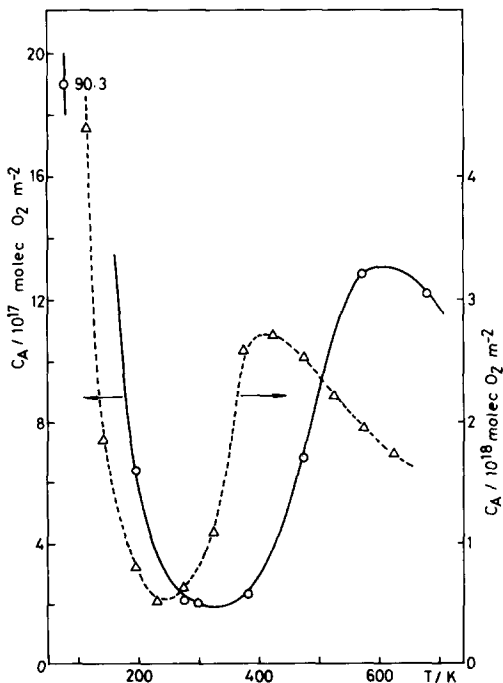


FIG. 5. Isobars for total adsorption at  $6.7 \times 10^3 \text{ Nm}^{-2}$ ; (—)  $O_2/\text{LaCrO}_3$ , (---)  $O_2/\text{LaCoO}_3$ .

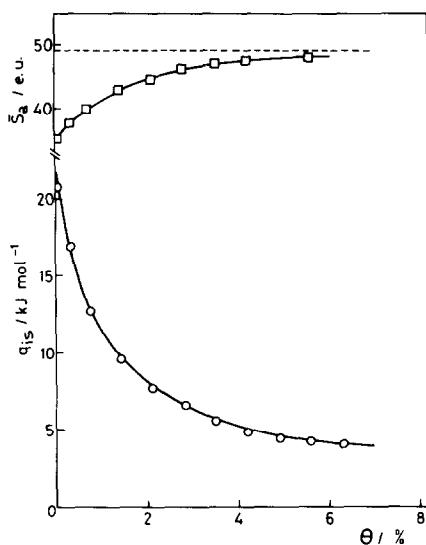


Fig. 6. Isosteric heats (○) and entropies (□) of adsorption obtained from reversible isotherms. (---) Entropy of the gaseous phase.

coverage equal to 1 could be in large error. Therefore the data were not fitted to the equilibrium equation of this model. Experimental entropies (Fig. 6) calculated from reversible isotherms (195–273 K) (11) are very near to the entropy of the gaseous phase. This also shows that this reversible adsorption is physisorbed.

### Reducibility

In Table 3, data of reducibility with H<sub>2</sub> are given. They indicate a high stability of the Cr<sup>3+</sup> ion in the perovskite structure. Considering only the surface layer of metal ions and assuming a density of  $6.7 \times 10^{18}$  Cr<sup>3+</sup> ions per square meter (equal to that calculated for LaCoO<sub>3</sub>, taking the planes of lower Miller's index as the most frequently exposed), a reduction level of 1 *e*<sup>-</sup> per molecule on the surface is attained at 1170 K (column 3); above this temperature, bulk reduction starts; nevertheless at 1270 K, the highest temperature studied, this reduction amounts only to  $1.30 \times 10^{-2}$  *e*<sup>-</sup> per molecule, column 4). Such behavior is in marked contrast with that observed by Crespin and Hall (9) for LaCoO<sub>3</sub>. This ox-

ide underwent a bulk reduction of 1 *e*<sup>-</sup> per molecule at 673 K and 3 *e*<sup>-</sup> per molecule at 773 K. Also, LaCrO<sub>3</sub> is the oxide of lower reactivity with CO, within the series LaMeO<sub>3</sub>; while in the surface of the perovskite where *Me* = Mn, Fe, or Co clear bands of carbonates were observed after adsorption of CO at r.t., in the system CO/LaCrO<sub>3</sub> at r.t. only a weak band at 1650 cm<sup>-1</sup>, of a bidentate carbonate, was detected (8).

### Kinetics of Adsorption

*Effect of temperature.* The integral kinetic results (*C<sub>A</sub>* vs *t*) at a constant pressure ( $6.7 \times 10^3$  N m<sup>-2</sup>) obtained in the temperature interval 373–777 K are plotted in Fig. 7). The kinetic isobar shows an increase in adsorbed amount with temperature and a maximum at 620 K; this is in agreement with the isobar found from equilibrium data (Fig. 5) and confirms the activated character of oxygen adsorption between 350 and 600 K. Therefore the analysis of these data was made according to the Elovich's equation,

$$\frac{dC_A}{dt} = a \exp(-b C_A) \quad (1)$$

or in its integrated form,

$$C_A = \frac{1}{b} \ln(ab) + \frac{1}{b} \ln(t + t_0) \quad (2)$$

TABLE 3  
Reduction of LaCrO<sub>3</sub> in H<sub>2</sub>

<i>T</i> (K)	$\Delta W_{O_2}^a$ (mg g <sup>-1</sup> )	<i>N</i> <sub>1</sub> <sup>b</sup> ( <i>e</i> <sup>-</sup> molec <sup>-1</sup> )	<i>N</i> <sub>2</sub> <sup>c</sup> ( $\times 10^{-3}$ <i>e</i> <sup>-</sup> molec <sup>-1</sup> )
670	0.119	0.36	3.5
870	0.167	0.51	5.0
970	0.219	0.67	6.6
1070	0.274	0.84	8.2
1170	0.333	1.02	10.0
1270	0.436	1.34	13.0

<sup>a</sup> Weight loss in mg per g of sample.

<sup>b</sup> Electrons per molecule assuming surface reduction ( $6.7 \times 10^{18}$  LaCrO<sub>3</sub> molecules per m<sup>2</sup>).

<sup>c</sup> Electrons per molecule assuming bulk reduction.

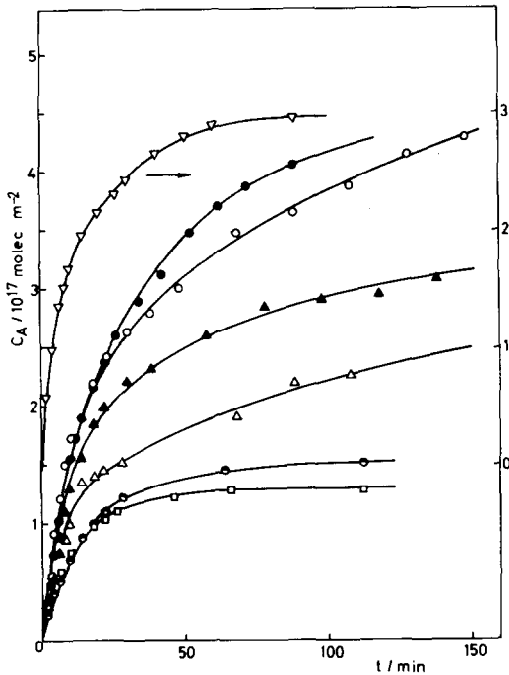


FIG. 7. Integral kinetic data of adsorption at  $6.7 \times 10^3 \text{ N m}^{-2}$  and different temperatures.  $\square$ , 373;  $\bullet$ , 425;  $\triangle$ , 479;  $\blacktriangle$ , 521;  $\circ$ , 573;  $\bullet$ , 620;  $\nabla$ , 777 K.

where  $C_A$  is the amount adsorbed at time  $t$ ;  $a$ ,  $b$ , and  $t_0$  are constants. If the adsorption process obeys Eq. (1) from the beginning the condition  $C_A = 0$  at  $t = 0$  applies and,

$$t_0 = \frac{1}{a b} \quad (3)$$

The applicability of Eq. (3) can be easily tested, and in our case it was not obeyed. To account for this discrepancy the assumption of a pre-Elovichian adsorption was made. Aharoni and Ungarish (12) have developed a simple method for obtaining  $t_0$  objectively from experimental data without making any assumption about this pre-Elovichian process. By differentiating Eq. (2) the following equation results,

$$t = Z(t)/b - t_0 \quad (4)$$

where  $Z(t)$  is the reciprocal of the adsorption rate. Extrapolation of the linear part of  $t$  vs  $Z(t)$  plots to  $Z(t) = 0$  gives directly  $t_0$ . The  $t$  vs  $Z(t)$  curves corresponding to the family of kinetic runs in Fig. 7 are given in Fig. 8. The  $t_0$  values determined from these are given in Table 4 (column 2). From the

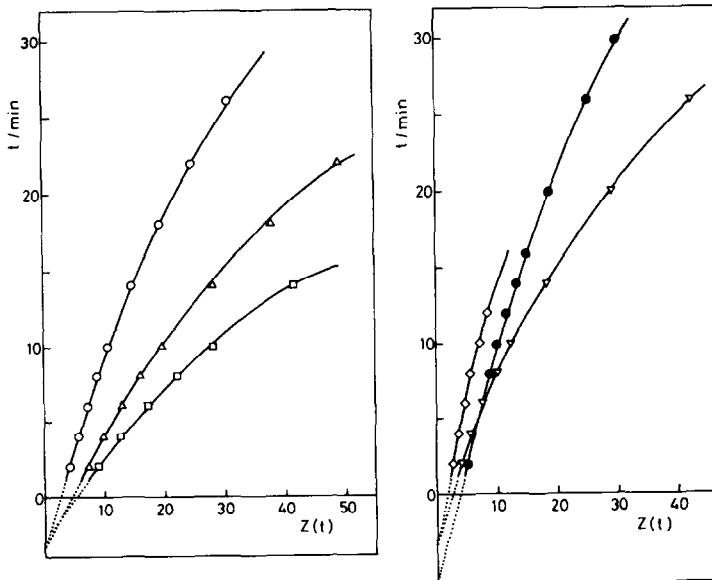


FIG. 8. Plots of  $t$  (time) vs  $Z(t)$  (reciprocal of the adsorption rate) at  $6.7 \times 10^3 \text{ N m}^{-2}$ .  $\square$ , 373;  $\triangle$ , 479;  $\circ$ , 573;  $\bullet$ , 620;  $\diamond$ , 670;  $\nabla$ , 777 K.

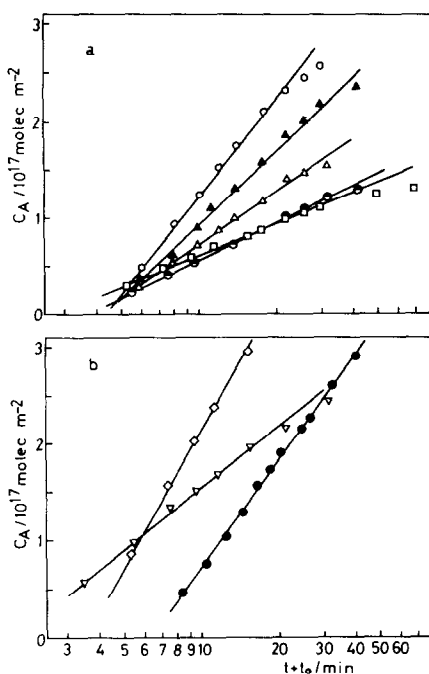


FIG. 9. Elovich's plots of  $C_A$  vs  $\ln(t + t_0)$  at  $6.7 \times 10^3$  N m<sup>-2</sup>. (a)  $\square$ , 373;  $\bullet$ , 425;  $\triangle$ , 479;  $\blacktriangle$ , 521;  $\circ$ , 573 K. (b)  $\bullet$ , 620;  $\diamond$ , 670,  $\nabla$ , 777 K.

slope of semilogarithmic plots  $C_A$  vs  $\ln(t + t_0)$  of Eq. (2) (at  $6.7 \times 10^3$  N m<sup>-2</sup> and 373–777 K) (Fig. 9),  $b$  values were calculated (Table 4, column 4). They decrease with increasing temperature as it can be expected when activated adsorption occurs.

**Activation energy.** The apparent activation energy of adsorption ( $E_a$ ) was calculated by means of plots  $\ln r_0$  (initial rate of

adsorption at  $t = 0$ ) vs  $1/T$  (Fig. 10) from which a value of 16.4 kJ mol<sup>-1</sup> was found.  $E_a$  can also be calculated by means of plots  $\ln b$  vs  $1/T$  (13) ( $b$ , Elovich's preexponential coefficient). To show the differences in  $E_a$  when these two methods are used, a plot of  $\ln b$  vs  $1/T$  ( $b$  values were taken from Table 4) was included in Fig. 10; from its slope an activation energy of adsorption significantly lower (9.7 kJ mol<sup>-1</sup>) than that obtained from initial rates of adsorption was found; the effect of  $\theta$  on  $E_a$  is clear (14) as  $b$  values were calculated from plots  $C_A$  vs  $t + t_0$  (see above) where  $0 \leq t \leq 150$  min.

It should be noted that this type of calculations should be used only in the ascending branch of the isobar (activated zone). This point has been commented by us in an earlier work (15). The anomalous  $E_a$  values found by Taylor and Liang (16) for H<sub>2</sub> adsorption on ZnO and also the successive stages found by Low (17) in the kinetic curves of the same adsorption system have a common origin in the occurrence of different adsorption processes when large temperature zones are considered.

**Effect of pressure.** Integral kinetic data  $C_A$  vs  $t$  at constant temperature (673 K) and variable pressure ( $2.8 \times 10^3$  to  $2.6 \times 10^4$  N m<sup>-2</sup>) are plotted in Fig. 11. For  $t \leq 5$  min., the curves overlap but at larger  $t$  a clear effect of pressure appears. Initial adsorp-

TABLE 4

Kinetic Parameters for Isobaric Runs			
$T$ (K)	$t$ (min)	Slope	$b$
373	3.2	0.474	2.11
425	3.5	0.556	1.80
479	3.8	0.764	1.31
521	3.9	1.148	0.87
573	4.0	1.375	0.73
620	6.4	1.586	0.63
670	3.4	1.945	0.51
777	1.5	0.884	1.13

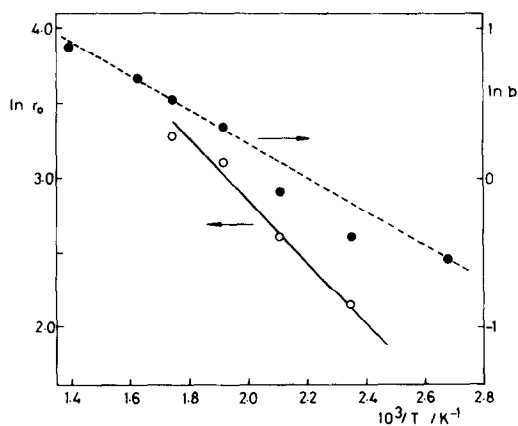


FIG. 10. Arrhenius plots of initial adsorption rate,  $r_0$  (O) and constant  $b$  of Elovich's equation (●) vs  $1/T$ .

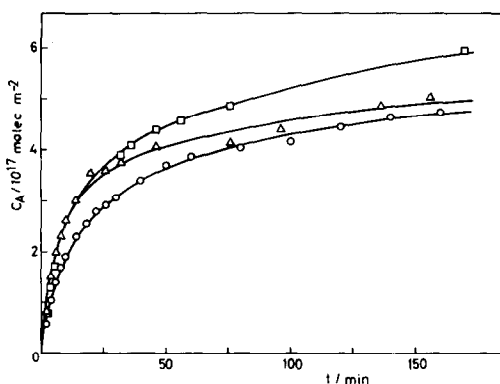


Fig. 11. Integral kinetic data of adsorption at 673 K and different pressures.  $\circ$ ,  $2.8 \times 10^3$ ;  $\triangle$ ,  $3.8 \times 10^3$ ;  $\square$ ,  $2.6 \times 10^4$  N m<sup>-2</sup>.

tion rates were plotted in Fig. 12. As it can be observed, a linear dependence between  $r_0$  and  $P$  holds at pressures below  $3 \times 10^3$  N m<sup>2</sup>. This suggests a Langmuirian behavior for the system O<sub>2</sub>/LaCrO<sub>3</sub> at low pressures as  $r_0 = a = k_a P$  ( $a$ , constant of Elovich's equation;  $k_a$ , adsorption constant) for  $t = 0$ . From the plot  $r_0$  vs  $P$ , a value for  $k_a$  of  $2.4 \times 10^{-4}$  N<sup>-1</sup> m<sup>2</sup> min<sup>-1</sup> was found. In a previous work, a linear dependence of  $r_0$  vs  $P$  in the whole pressure interval studied ( $5 \times 10^2$  to  $1.5 \times 10^4$  N m<sup>-2</sup>) was found for the system CO/LaCrO<sub>3</sub> (15). However, the adsorption constant for CO ( $9.4 \times 10^{-6}$  N<sup>-1</sup> m<sup>2</sup> min<sup>-1</sup>) was remarkably lower than that for O<sub>2</sub>.

#### Oxygen Adsorption and Catalytic Activity

As it can be observed by comparison of the adsorption isobars at 50 mm Hg in Fig. 5, there is a marked difference between the oxygen adsorption on LaCrO<sub>3</sub> and on LaCoO<sub>3</sub>. In the interval 300 to 500 K, the adsorption on the latter is higher by a factor of 3 to 9 over the adsorption on the former. Also the adsorption kinetics for O<sub>2</sub> is faster on LaCoO<sub>3</sub>. On the other hand the activation of the O<sub>2</sub> molecule (indicated by the ascending branch of the isobar) on LaCoO<sub>3</sub> starts at a lower temperature (250 K) than that on LaCrO<sub>3</sub> (350 K). On the system O<sub>2</sub>/LaCoO<sub>3</sub> this activation was shown (by ESR) to be related to the dissociative adsorption of oxygen as O<sup>-</sup> on the transition

metal ion (1). These factors can account for the higher catalytic activity for CO oxidation of LaCoO<sub>3</sub> as compared to that of LaCrO<sub>3</sub>.

The low coverages attained at temperatures where the chemisorption is predominant (Table 2) indicate that a rather small fraction of the oxide surface is active. This shows that the oxygen adsorption takes place only on surface defects as transition metal ions in highly reactive position (corners, edges), anion vacancies, etc. According to Iwamoto *et al.* simple oxides whose metal ion has a  $d^0$  or  $d^{10}$  configuration are poor adsorbents of oxygen (groups A and C in Ref. (3)). Therefore the La<sup>3+</sup> ion should not play an important role as adsorption center.

LaCoO<sub>3</sub>, more easily reducible (and therefore with higher mobility of oxygen) than LaCrO<sub>3</sub> showed a higher activity for CO oxidation (2). Likewise, in a previous work (8) it was found that the reactivity of perovskite-type oxides with CO followed the same sequence than that observed in the catalytic activities for CO oxidation: LaCoO<sub>3</sub> > LaFeO<sub>3</sub> > LaCrO<sub>3</sub>. Similar results have been given by van Damme and Hall (18) in a recent study on LaCoO<sub>3</sub>, SrTiO<sub>3</sub> and BaTiO<sub>3</sub>. Also the differences in concentration of hydroxyl groups found after H<sub>2</sub>O adsorption on LaCrO<sub>3</sub> (Fig. 3) and LaCoO<sub>3</sub> (9) can be assumed to be related to the higher reducibility of the latter, i.e., to its easier formation of oxygen vacancies.

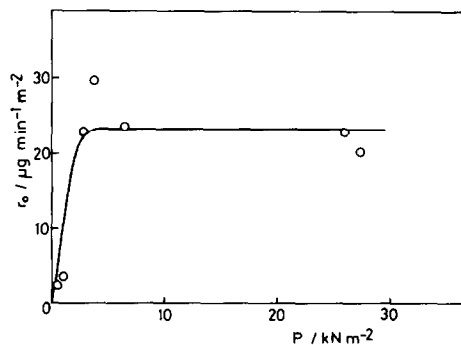


Fig. 12. Effect of pressure on the initial adsorption rate,  $r_0$ .

Meadowcroft (19) showed that LaCoO<sub>3</sub> has a high electrocatalytic activity for O<sub>2</sub> reduction and LaCrO<sub>3</sub> is not active. According to this author this difference may be due to the fact that LaCrO<sub>3</sub> is a *p*-type semiconductor while LaCoO<sub>3</sub>, besides having a small band gap, can easily be made either *p*-type or *n*-type semiconductor. The amphoteric character of this last oxide could account for its high oxygen adsorption and ready reducibility.

The results reported here are in agreement with those of Iwamoto *et al.* (3) who found fair correlations amongst heat of formation of transition metal oxides, oxygen adsorption and catalytic activity for total oxidation, i.e., the less stable oxides (and therefore those which more readily form surface defects) exhibited both higher oxygen adsorption and higher catalytic activity.

## REFERENCES

1. Tascón, J. M. D., and González Tejuca, L., *Z. Phys. Chem. Neue Folge* **121**, 63, 79 (1980); *J. Chem. Soc. Faraday Trans. 1* **77**, 591 (1981).
2. Tascón, J. M. D., and González Tejuca, L., *React. Kinet. Catal. Lett.* **15**, 185 (1980); Tascón, J. M. D., Mendioroz, S., and González Tejuca, L., *Z. Phys. Chem. Neue Folge* **124**, 109 (1981).
3. Iwamoto, M., Yoda, Y., Yamazoe, N., and Seiyama, T., *J. Phys. Chem.* **82**, 2564 (1978).
4. Johnson, Jr., D. W., Gallagher, P. K., Schrey, F., and Rhodes, W. W., *Amer. Ceram. Soc. Bull.* **55**, 520 (1976).
5. Courty, Ph., Ajot, H. Marcilly, Ch., and Delmon, B., *Powder Technol.* **7**, 21 (1973).
6. Tofield, B. C., and Scott, W. R., *J. Solid State Chem.* **10**, 183 (1974).
7. Voorhoeve, R. J. H., Remeika, J. P., and Trimble, L. E., *Ann. N.Y. Acad. Sci.* **272**, 3 (1976).
8. González Tejuca, L., Rochester, C. H., Fierro, J. L. G., and Tascón, J. M. D., submitted for publication.
9. Crespín, M., and Hall, W. K., *J. Catal.* **69**, 359 (1981).
10. Emmett, P. H., "Catalysis," Vol. 1, p. 38. Reinhold, New York, 1954.
11. Rosynek, M. P., *J. Phys. Chem.* **79**, 1280 (1975).
12. Aharoni, C., and Ungarish, M., *J. Chem. Soc., Faraday Trans. 1* **72**, 400 (1976); **73**, 456, 1943 (1977).
13. Leibowitz, L., Low, M. J. D., and Taylor, H. S., *J. Phys. Chem.* **62**, 471 (1958).
14. Ungarish, M., and Aharoni, C., *J. Chem. Soc., Faraday Trans. 1* **79**, 119 (1983).
15. Fierro, J. L. G., and González Tejuca, L., *J. Colloid Interface Sci.* **96**, 107 (1983).
16. Taylor, H. S., and Liang, S. C., *J. Amer. Chem. Soc.* **69**, 1306 (1947).
17. Low, M. J. D., *Canad. J. Chem.* **37**, 1916 (1959).
18. van Damme, H., and Hall, W. K., *J. Catal.* **69**, 371 (1981).
19. Meadowcroft, D. B., *Nature (London)* **226**, 847 (1970).